A CONVEX OPTIMIZATION BASED APPROACH TO REDUCE EXTERNAL NOISE FROM PMRI IMAGES

Ifat Al Baqee

***Abstract*—**Parallel Magnetic Resonance imaging (pMRI) methods enable lessening of the MRI scanning time via simultaneous acquisitions of the k-space data. Noise, both external and internal, are an inherent research focus for parallel MRI (pMRI) scientists and engineers. Though many software based methods have been developed in recent years for reducing internal or reconstruction noise. External or physical noise is actually mostly tackled by hardware based approach. This work is a result for opting a software based solution to minimize external or physical noise through a convex optimization based approach with total variation or TV norm. Simulated results using manually generated noisy brain data and scanned phantom in noisy environment have been shown in this paper. As, simulating popular hardware controlled noise enhancement algorithms is out of scope for this work, software simulated results from some popular algorithms will be compared at the end of this paper. Hopefully, the promising results of this work is going to provide a significant contribution for researchers working in related fields.

***Keywords*—**g-maps, standard deviations, GRAPPA, SENSE, SPIRiT, iterative optimization, convex optimization, sum-of-square, artifacts

I. INTRODUCTION

THE accumulation of noise in parallel MRI or pMRI reconstruction has always been a vital issue for imaging assessment by healthcare professionals. Accelerated multichannel pMRI is often susceptible to various types of internal and external noises. Where, internal noise is actually demarcated by accumulated noise during pMRI reconstruction process and is actually caused by the non-linearity of reconstruction algorithms [1], [2]. In author's previous work [3], a detailed comparison between different popular algorithms in the basis of reconstruction noise performances had been presented. pMRI reconstruction methods like [4] and [5] employ some degree of variation normalization to tackle the reconstruction noise. However, most of the reconstruction algorithms can't handle the noise which is already added to the scanned data, more specifically can be mentioned as external or hardware noise. The objective of this paper is to investigate the types of external noise factors and to develop an algorithm based on [4] to improve the signal-to-noise or SNR performance of pMRI images contaminated by external noise.

The magnetic resonance image reconstructed by parallel coil array is complex and proportional to the proton density of the object, the external magnetic field and the radio frequency excitation pulses. The sensitivity functions of the scanner coils are also complex valued [6]. From the theory of MRI physics, it is understandable that external noise targets three factors during image scanning. The first factor which can develop external interferences is mostly a living being such as a human subject. MRI subject can produce breathing artifacts, motion blurs or acoustic noises, though this type of noise can be manually minimized. The two factors which greatly contribute to the external noise are the inhomogeneity in external magnetic field and radio frequency or RF interference in the RF excitation pulses [2]. Mostly, acoustic noises from surrounding environment are the primary donor for RF interferences [7]. Regular servicing and maintenance of coil arrays can mostly diminish the noise due to inhomogeneity. There is a bonus factor which also contribute to external noise up to some extent is thermal. But modern machineries are kept in well air-conditioned facility which actually helps in this regard. In this work, focus is given on various types of noises due to RF interference and a method has been proposed to minimize those.

The noise due to external RF interferences can be divided into three types on the basis of their mathematical property; Rician noise, Gaussian Noise and Rayleigh noise [8]. However, if the SNR value of the reconstructed pMRI image exceeds '2', Rician distribution converges into Gaussian distribution and when it is down to '0', it behaves like Rayleigh distribution. As SNR around the center of a magnitude only MR image is more than '2', it becomes Gaussian distribution and behaves like Rayleigh distribution in the area far from the center [9]. Several de-noising algorithms have been proposed but mostly those deal with the Rician distributions [8]. The primary sources of RF interferences are mainly caused by three things: electronic interventions in the RF receiver circuits, Radiofrequency emissions due to subject aka patient's body temperature and from the leakage signals generated from machine's own trans-receiver circuits. Noise in pMRI produces random oscillations, which decreases the image contrast due to signal dependent data bias. This hampers the accurate qualitative and quantitative evaluation as well as feature detection of images. As the SNR of pMRI is mostly high in most of the clinical applications, added external noise is mostly established into Gaussian noise distribution [10].

There are several key de-noising algorithms developed to tackle various types of MRI noises. These noise reduction methods can be categorized into linear and non-linear sects. In

Dr. I. A. Baqee is with the Department of Electrical and Electronic Engineering, Southeast University, Dhaka, Bangladesh (e-mail: *ifat.albaqee@seu.edu.bd*).

linear algorithms, noise is minimized by updating pixel value from weighted average of neighborhood but reduces the quality of an image whereas in non-linear algorithms deal with edge detection and preservation but the fine resolution is degraded. Some of the popular linear filtering methods are Markov Random Field model [11], anti-isotropic diffusion filtering [12]-[13], wavelet based de-noising algorithms [14]-[15]. Also, some non-linear methods are [16], bi-lateral and tri-lateral filtering [17] and spectral subtraction method [18] which can give up to 40% better SNR but with the expense of computation load.

In this work, a convex optimization method has been proposed with total variation penalties. The method is non-linear so can provide better SNR results as well it has less computational burden. The method is tested with a noise contaminated phantom data and a simulated noisy brain data to show the efficiency of the proposed method. The standard deviations as well as the SNR for every reconstructed scenario is also calculated for proper demonstration.

II. Theory and Methodology

In this section, an algorithm to reduce external noise based on convex optimization based approach is proposed. In author's previous work [4], it has been already shown that the proposed convex solution space based algorithm can reduce the reconstruction noise substantially. This work is also based on that proposed convex hull based solution approach with some added normalization penalty which works efficiently on external noise.

As discussed above, external noise in MRI can be categorized into Rician, Gaussian and Rayleigh distribution, though after inspecting the MRI pixel value patterns it can be also assumed that around the center axis space the pixel magnitude distributions act like Gaussian pattern. In [5], it has been shown that adding total variation or TV penalties is a very effective approach to minimize Gaussian noise. In this work, the previous convex optimization based approach in [19] and [4] is modified with TV norm for better external noise performance.

pMRI reconstruction algorithms can be classified into two principle genres. One major methods tend to rely on the coil sensitivity data mainly. These methods approximate the coil sensitivity data through a reference scan or some kind of iterative optimizations, which afterwards is used to generate the final pMRI image. The foremost algorithm of this category is SENSE [6] and its major extensions like iterative SENSE, JSENSE [20] etc. Coil sensitivity estimation is a vital part of these methods otherwise the results can be spoiled by artifacts and noise. The other category of methods relies on auto-calibration data and opts for a coil-by-coil image reconstruction step and then reconstruct the final image through some kind of coil data combination technique. Notable methods in this class are GRAPPA [21] and it's extensions. In [4], the reconstruction method has been divided into two parts as it falls into the second principle category of pMRI reconstruction algorithms.

In this paper, the proposed method also follows the footstep of the convex hull based solution approach as in [4]. But there are few necessary modifications is done as this work mostly deals with the external noise interferences. The compressed sensing based approach in [22] assumes that pMRI images are sparse in a certain transform domain like Fourier domain or k-space domain. Sparsity characteristics greatly enhances the possibility that added noise data is distributed across the whole image space whereas the true image data is distributed mostly around the center of the k-space. It is shown in [seu1] that the application of compressed sensing in dual-step optimization method [23] greatly promote the accuracy in reconstructed pMRI image as well as adding variational penalty like TV norm works effectively to reduce redundant reconstruction noise.

In this work, the proposed coil-by-coil reconstruction method in [23] is used in the first step of reconstruction.

$$\min_{\boldsymbol{z}} \|\boldsymbol{F}\boldsymbol{z} - g\|_2^2 + \frac{\alpha}{2}\|\boldsymbol{z}\|_{BV} + \frac{\beta}{2}\|\boldsymbol{W}\boldsymbol{z}\|_1 \qquad (1)$$

where, $g \in \mathbb{C}^M$, is the scanned undersampled k-space pMRI data in its vector form, $\mathbb{C}$ represents the complex form. $\boldsymbol{z} \in \mathbb{C}^{LN^2 \times 1}$, reconstructed coil-by-coil image data in vector form. L represents the number of coils used during the pMRI scanning. $\boldsymbol{F}\mathbb{C}^{M \times LN^2}$ represents the undersampled Fourier space domain. $\|\boldsymbol{W}\boldsymbol{z}\|_1$ is the L1 penalty on $\boldsymbol{z}$ to promote the sparsity [22] and $\boldsymbol{W}$ represents the wavelet transform domain. $\| \ \|_{BV}$ represents Besov [24] norm which is actually the variational penalty. Interested readers can go through [22] and [22] more details on this method.

Assuming that the final combined image from each coil is magnitude only as in methods like [21], a convex solution space based approached has been proposed in [4]. Let's assume that $z_{\boldsymbol{ml}} \in \mathbb{C}^{N^2 \times 1}$ is the matrix form derived from the solution in (1). Let $I_m \in {\mathbb{R}_+}^{N \times N}$ be the magnitude of the final image to be reconstructed. Since the magnitudes of coil sensitivities are bounded due to bounded inductances of the coils, there exist constant entity $B_l \in {\mathbb{R}_+}^{N \times N}$, such that $|\boldsymbol{z}| \preccurlyeq B$ for each coil $l = 1, 2, \ldots, L$. It follows that

$$|z_{\boldsymbol{ml}}| \preccurlyeq B_l \odot I_m, \qquad for\ l = 1, 2, \ldots, L \qquad (2)$$

If I_m and $z_{\boldsymbol{ml}}$ are reflected as the solution variables, the inequalities (2) form a convex hull containing the solutions of I_m and $z_{\boldsymbol{ml}}$, with properly chosen constant bound vectors B_l.

Choosing the boundary matrix can be delicate, but putting an element-wise positive penalty with initial approximation on estimated weights Z can lead to a suitable B.

$$min_{B,\tau}\|B - \boldsymbol{z} - \tau\|_2^2, \ \ s.t. \ \ \tau \succcurlyeq 0 \qquad (3)$$

Approximating B for each coil in (3) converts problem (2) into no longer bi-linear. Assuming the final MR image I_m to be sparse in certain transform domain as well as non-negative, following optimization scheme has been suggested

$$\min_{I_m^0} \|I_m\|_1$$
$$subject\ to: I_m \succcurlyeq 0, |z_{\boldsymbol{ml}}| \preccurlyeq B_l \odot I_m \qquad (4)$$

The total Gaussian variational penalties or TGV norm used in [irgn] proved to be very effective in tackling Gaussian noise. The unconstraint Lagrangian form of the L_1 regularized optimization problem (4) along with additional variational

penalty can be written as

$$\min_{I_m^0, q_l} \frac{1}{2}\|B_l \odot I_m - |z_{ml}| - q_l\|_2^2 + \frac{\gamma}{2}\|I_m\|_1 + \frac{\delta}{2}\|I_m\|_{TGV}$$
$$subject\ to: I_m \succcurlyeq 0, q_l \succcurlyeq 0 \qquad (5)$$

Where, $q_l \in \mathbb{R}_+^{LN\times N}$ is a non-negative element-wise penalty to push $|z_{ml}|$ always within the boundary of the convex solution space. The output quality of the proposed formulas mostly depends on the $\|\ \|_{TGV}$ penalty. Perhaps, the advantage of this TGV norm is it promotes the normalization of Gaussian variation. As the nature of the significant portion of the external interferences are Gaussian, hopefully this formulation is going to benefit the noise reduction in pMRI images. In the upcoming sections, experimental setups and results using the combination of formulas proposed in (1) and (5) is going to be discussed.

III. Experimental Setup And Results

Two different types of dataset have been applied to test the noise performance of the proposed method. In this experiment, the objective is to test a dataset which is contaminated by some degree of external white noise. Adding additional noise for test purpose exhibits one more issue to deal with. When an in-vivo data from a human subject is scanned, adding external noise can be harmful for the subject's health, which is an unsure case. But for real time experiments, a phantom dataset is scanned which is going to be contaminated by external noise from white noise signal generator device.

A. Data Acquisition

The first dataset is a single slice brain data set of a healthy human volunteer subject; the dataset is also available in [25]. The dataset was scanned by a 3 Tesla SIEMENS Trio scanner with an eight-channel head array and an MPRAGE (3D Flash with IR prep.) sequence. The parameters of the scan were TR, TE = 2530, 3.45 milliseconds, TI = 1100 milliseconds, flip angle = 7^0, image resolution is 256 by 256, thickness of object slice is 1.33 mm and FOV =FOV is 256 by 256 mm^2. After acquisition of the dataset, white Gaussian noise is added. For this purpose, a noise matrix has been designed which has the same resolution as the scanned dataset of each coil. The noise matrix is denoted by $n_l \in \mathbb{C}^{N\times N}$, where l=1, 2, 3.., L represents the array coil sequence. The generated noise matrix is Gaussian in nature and after linearly adding to the full dataset the mean variance or standard deviation is 1.53%. The full set of attained k-space data are manually and uniformly undersampled at the nominal acceleration rate, denoted by f_{nom}, along with additional 36 extra auto-calibration signal (ACS) lines in the central k-space region along the phase encoding direction to form the undersampled k-space data pattern. Two sets of undersampled data at f_{nom} = 4 and 8 have been obtained. Taking into account the additional 36 ACS lines, the corresponding net undersampling rates, denoted by f_{net}, of the datasets are f_{net} = 2.56 and 3.76 respectively. It is also worth to be noted that the noise matrix n_l was Fourier transformed to k-space data before linearly added to the fully sampled k-space data.

Now for the second dataset as there is no health risk while scanning of a non-living object, external white noise generator device has been implemented during the scanning process. The second data of a phantom was acquired on a 3 Tesla SIEMENS scanner with a 4-channel head with true fast imaging with steady state precession sequence (TrueFISP). The parameters of the scan were TR by TE = 11 by 6.5 milliseconds, image size of N×N = 256 × 256, flip angle = 60^0 and field of view or FOV = 162 × 162 mm^2. White Gaussian noise generator device or WGN made by dB corp. [26] was used during the scanning process to simulate acoustic noisy environment. The acquired k-space data is in the Cartesian coordinate system and uniformly undersampled at the nominal rate of f_{nom} = 4, 8 and 12. The undersampled data together with the 32 extra ACS lines in the central k-space region along the phase encoding direction generating a undersampled k-space dataset with net undersampling rate f_{net}= 2.67, 4 and 4.73.

In addition to rectangular undersampling, both datasets have been undersampled using a radial pattern too. Radial pattern is used to give a good insight about the distribution characteristics of external noise pattern. Both the undersampling pattern is demonstrated in Fig. 1 and Fig. 2.

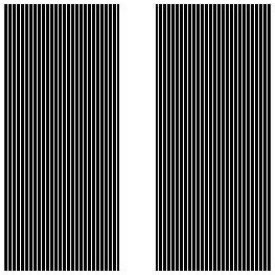

Fig. 1. USACS or rectangular undersampling pattern with f_net =2.56 (f_nom = 4)

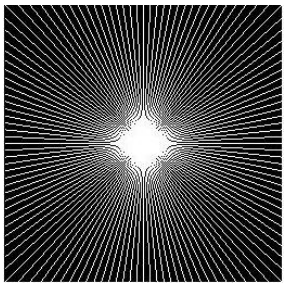

Fig. 2. Radial under sampling pattern

B. Computational Setups

The proposed computational algorithm for pMRI reconstructions has been simulated by MATLAB (Math-Works, Natick, MA, USA). the normalized mean square error of the reconstructed image I_m is defined as

$$e_{NMSE} = \frac{\|I_m - I_{SOS}\|^2}{\|I_{SOS}\|^2} \qquad (6)$$

Where, I_{SOS} is the reconstructed image from the fully sampled dataset. Sum-of-square or SOS operation has been performed to combine the coil images from multiple coils into a single final one [21].

The process to estimate the signal-to-noise ratio or SNR of the reconstructed images is a tricky one as there is no standard system for it. There are some established estimation processes

of SNR for reconstruction noise performance such as in [27], but determining SNR in case of manually added external noise is still not well established. But hopefully, researchers depend on the figurative approach to observe the reconstruction performance in case of added external interferences. In this work, the quality of the proposed method is observed through two ways, first will be the dependable figurative approach through generated pMRI images. Other is the calculation of standard deviation [3] for each reconstruction, as standard deviation can give some insight about SNR and noise in an image. As the standard deviation increases, it is generally assumed that noise is getting worse or SNR is decreasing.

C. Results and Analysis

The contaminated in-vivo brain data with added Gaussian noise with a variance of 1.53% is shown in Fig. 3.

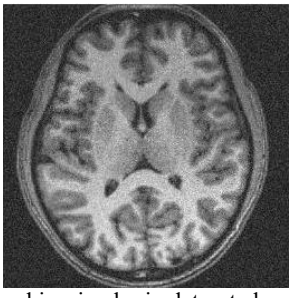

Fig. 3. Fully acquired in-vivo brain dataset along with added white Gaussian noise

Fig. 3 depicts a scenario what a pMRI image can look in case of environmental acoustic and thermal noise. Though not 100% accurate, it's a simulated lookup into magnetic resonance image performance in case of external noise. Now, after implementing the proposed algorithms in equations (1) and (5), the reconstructed results are shown in Figs. 4-5.

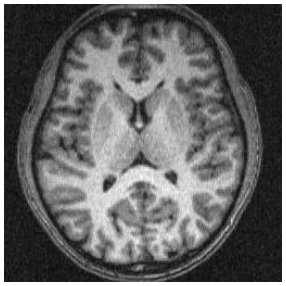

Fig. 4. Reconstructed in-vivo brain image for rectangular under sampling pattern with f_{nom} = 4

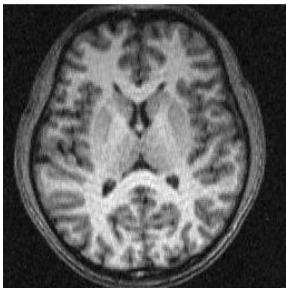

Fig. 5. Reconstructed in-vivo brain image for rectangular under sampling pattern with f_{nom} = 8

It's very clear from the comparison between images that in the reconstructed images of Fig. 4 and 5, the noise has been visibly improved. Though in Fig. 5 there are some visible artifacts but that is due to the higher acceleration rate f_{nom} = 8. Although there are still some visible substances of noise left, but in real time scenario external noises don't have high variances like 1.53%. the purpose of the simulation is to depict a clear figurative comparison that the proposed formula in this work has a contribution in reducing added noise. Readers also should note that modern pMRI scanning system still does not cross nominal acceleration rate that '4'. So it's safe to say that the proposed technique can subsidize external noise as well as maintain quality of reconstruction.

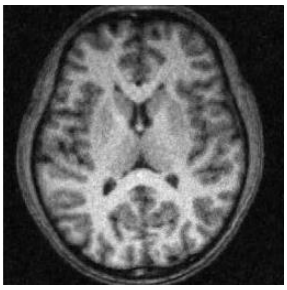

Fig. 6. Reconstructed in-vivo brain image for radial under sampling

Another interesting insight can be seen from Fig. 6. Where the fully sampled noisy was undersampled using radial pattern. The visible noise performance is better than that of Fig. 4. The reason is because radial pattern behaves somehow like Gaussian distribution, where center has larger values compare to outer regions where values become sparser. Radian undersampling greatly helps picking the external noise pattern in case if it is Gaussian in nature and TGV norm in equation (5) greatly improves the variational stabilization to reduce noise from image.

The NMSE values and standard deviation for different undersampling pattern and different acceleration rates is given in Table I and II.

TABLE I
NMSE VALUES OF IN-VIVO BRAIN DATASET FOR DIFFERENT UNDERSAMPLING

UNDERSAMPLING TYPE	NMSE
RECTANGULAR (f_{nom} = 4)	0.0039
RECTANGULAR (f_{nom} = 8)	0.0072
RADIAL	0.0042

*Lower is Better

TABLE II
STANDARD DEVIATIONS (%) OF RECONSTRUCTED IN-VIVO IMAGES FOR DIFFERENT UNDERSAMPLING

UNDERSAMPLING TYPE	STANDARD DEVIATION (%)
RECTANGULAR (f_{nom} = 4)	0.56
RECTANGULAR (f_{nom} = 8)	0.97
RADIAL	0.36

*Lower is Better

For any image, standard deviation below '1%' is acceptable for MRI images. From both the tables it is clear that the standard deviation of the reconstructed pMRI images are in

acceptable range. The proposed formulas have reduced the standard deviation from 1.53% to below 1% which is a significant contribution.

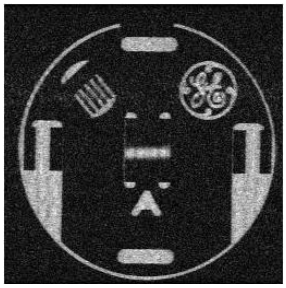

Fig. 7. Fully sampled noisy phantom data

Though simulated noise scenario testing through in-vivo data gives a narrow idea about the noise performance, the results from the noisy phantom data where the external noise was added in hardware basis and real time expectation-wise, would give more detail insight about the noise efficiency. Now let's have a look on the noisy phantom image acquired as described in section III.A, shown in Fig. 7. Now, after implementing the proposed formulas in equations (1) and (5), the reconstructed results are shown in Figs. 8-10.

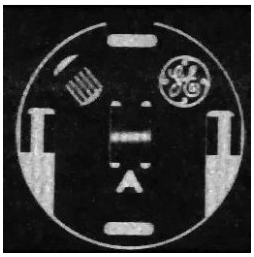

Fig. 8. Reconstructed phantom image for rectangular under sampling pattern with f_{nom} = 4

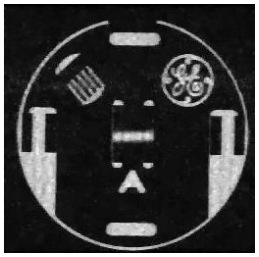

Fig. 9. Reconstructed phantom image for rectangular under sampling pattern with f_{nom} = 8

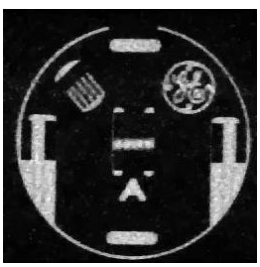

Fig. 10. Reconstructed phantom image for radial under sampling

From the results in Fig. 8 to Fig. 10, it is observed that the reconstructed phantom images follow the same pattern as the in-vivo brain images with added simulated noise. In Fig. 8 and Fig. 9, the difference between the reconstructed images is very minimal except Fig. 8 exhibits a little bit higher resolution. The reason is due to sparse nature in the phantom dataset, that is why increasing the undersampling rate has minimal effect on the quality of the reconstruction. Both results in Fig. 8 and Fig. 9 improves the noise substantially compare to Fig. 7. In Fig. 10, where the dataset was undersampled using radial pattern, provides the best result so far. As it is already mentioned that radian undersampling pattern greatly co-operates with the total Gaussian Variational penalties (TGV norm), which in turn has great impact on reducing external noise as well as retaining quality of the reconstructed images.

The NMSE values and standard deviation for different undersampling pattern and different acceleration rates is given in Table III and IV.

TABLE III
NMSE VALUES OF PHANTOM DATASET FOR DIFFERENT UNDERSAMPLING

UNDERSAMPLING TYPE	NMSE
RECTANGULAR (f_{nom} = 4)	0.0026
RECTANGULAR (f_{nom} = 8)	0.0046
RADIAL	0.0023

*Lower is Better

TABLE IV
STANDARD DEVIATIONS (%) OF RECONSTRUCTED PHANTOM IMAGES FOR DIFFERENT UNDERSAMPLING

UNDERSAMPLING TYPE	STANDARD DEVIATION (%)
RECTANGULAR (f_{nom} = 4)	0.38
RECTANGULAR (f_{nom} = 8)	0.72
RADIAL	0.31

*Lower is Better

As the standard deviation rate of the acquired noisy phantom data was originally measured '1.29', the improvements of the noise performance shown in Table IV are quite substantial. From the results shown above, it's pretty evident that the formulas proposed in this paper can offer a noteworthy addition to reduce external noise from pMRI images.

IV. CONCLUSIONS

RF interferences in MRI reconstruction has been a crucial area for researchers to deal with, as noise reduction algorithms often deal with poor reconstruction quality. That is why balancing between noise suppression and reconstruction quality has been an utter challenge for algorithm developers. Most of the linear and non-linear filter based approaches discussed in section I have some kind of reconstruction quality penalty [11]. The proposed formulas in this work has tried to minimize the external noise along with maintaining quality in the reconstructed images. From the results shown above, it is clear that though the noise optimization scheme can affect the resolution, but still it can maintain acceptable level of reconstruction error. It has already been shown in [4] that NMSE value of less than '0.0050' is considered as good quality of reconstruction for major pMRI methods. So, a decent standard for reconstruction quality as well as standard deviation less than acceptable range is an acknowledging factor that the proposed formulas are effective. Through comparison with other external noise reduction methods is

out-of-scope of this work, future study could be done on investigating the effectiveness of proposed method in comparison with other popular or state-of-art methods. The purpose of this work has been to formulate an algorithm to deal with external RF interferences, especially if the noise distribution factor embodies Gaussian Distribution. The efficiency and accuracy of the algorithm for the undersampled acquired k-space data have also been evaluated and shown in figurative as well as numerical depiction. Hopefully this work will give researchers a new approach of external noise reduction in pMRI and future study could be done to compare the method with other state-of-art algorithms and further improve it.

ACKNOWLEDGMENT

Author would intend to convey his gratitude to Dr. Kamlesh Pawer of Monash University Biomedical Imaging Laboratory (https://www.monash.edu/researchinfrastructure/mbi/home) for providing the raw noise contaminated phantom data which has been used in the experimentation without any copyright complaint.

REFERENCES

[1] F. A. Breuer, S. A. Kannengiesser, M. Blaimer, N. Seiberlich, P. M. Jakob, and M. A. Griswold, "General Formulation for Quantitative Gfactor Calculation in GRAPPA Reconstructions," *Magnetic Resonance in Medicine*, vol. 62, pp. 739–746, 2009.

[2] S. Aja-Fernández, G. Vegas-Sánchez-Ferrero, and A. Tristán-Vega, "Noise estimation in parallel MRI: GRAPPA and SENSE," *Magnetic Resonance Imaging*, vol. 32, pp. 281–290, 2014.

[3] I. A. Baqee, "A relative comparison of noise performances between different pMRI algorithms," *The SEU journal of Electrical and Electronic Engineering (SEUJEEE)*, vol. 1, issue. 1, pp. 1–6, 2021.

[4] I. A. Baqee, "A Novel Approach of Obtaining Optimal Solution for Iterative Self-Consistent Parallel Imaging Reconstruction," *International Journal of Scientific technology and research*, vol. 9, issue. 9, pp. 100–107, 2020.

[5] F. Knoll, C. Clason, K. Bredies, M. Uecker, and R. Stollberger, "Parallel imaging with nonlinear reconstruction using variational penalties," *Magnetic Resonance in Medicine*, vol. 67, pp. 34–41, 2012.

[6] K. P. Pruessmann, M. Weiger, M. B. Scheidegger, and P. Boesiger, "SENSE: Sensitivity encoding for fast MRI," *Magnetic Resonance in Medicine*, vol. 42, pp. 952–962, 1999.

[7] M. E. Ravicz, J. R. Melcher, and N. Y.-S. Kiang. "Acoustic noise during functional magnetic resonance imaging", *J Acoust Soc Am.*, vol. 108(4), pp. 1683–1696, 2000.

[8] B. Goyal, A. Dogra, S. Agrawal, and B.S.Sohi, "Noise Issues Prevailing in Various Types of Medical Images", *Biomedical & Pharmacology Journal*, vol. 11(3), pp. 1227–1237, 2018.

[9] "MR Quality Control: SNR, Nature and Characteristics of Noise," https://www.mriquestions.com/signal-to-noise.html, accessed in February 2021.

[10] B. Biswal, F. Z. Yetkin, V. M. Haughton, and J. S. Hyde, "Functional connectivity in the motor cortex of resting human brain using echo planar MRI", *Magnetic resonance in medicine*, vol. 34(4), pp. 537–541, 1995.

[11] S.Vaishali, K. K. Rao, and G. V. Rao, "A Review on Noise Reduction Methods for Brain MRI Images", 2015 International Conference on Signal Processing and Communication Engineering Systems, Guntur, India, 2015, pp. 363–365.

[12] M. A. Balafar, "Review of noise reducing algorithms for brain MRI images", *International Journal on Technical and Physical Problems of Engineering*, Vol. 4, Issue 13(4), pp. 54–59, 2012.

[13] P. Perona, and J. Malik, "Scale-space and edge detection using anisotropic diffusion", *IEEE transactions on Pattern Analysis Machine Intelligence*, vol.12(7), pp. 629-639,1990.

[14] F. Luisier, J. Patrick, and J.Wolfe, "Chi-Square unbiased risk estimate for denoising magnitude MR Images", IEEE International conference on image processing , pp. 1561–1564, 2011.

[15] X. Yang and B. Fei, "A wavelet multiscale denoising algorithm for magnetic resonance (MR) images", *Meas Sci.technol*, vol. 22, pp. 025803–025815, 2011.

[16] A. Buades A, B. Coll, and J. Morel, "A non-local algorithm for image denoising", IEEE computer society conference pon computer vision and pattern recognition, pp. 60–65, 2005.

[17] S. Prima, O. Commonwick, "Using bilateral symmetry to improve non-local means denoising of MR brain images", IEEE International symposium on biomedical imaging: From Nano to Micro, pp.1231–1234, 2013.

[18] M. A. Erturk, P. A. Bottomley, and A. M. E.-Sharkawy, "Denoising MRI using spectral subtraction", *IEEE Transactions on biomedical engineering*, vol.60(6), pp.1556–1562, 2013.

[19] Ifat-Al-Baqee, Cishen Zhang and Xin GAO, "Optimal parallel MRI reconstruction over a convex solution space", 2015 IEEE International Conference on Signal Processing, Communications and Computing (ICSPCC), pp. 736-739, 2015.

[20] L. Ying and J. Sheng, "Joint image reconstruction and sensitivity estimation in SENSE (JSENSE)," *Magnetic Resonance in Medicine*, vol. 57, pp. 1196–1202, 2007.

[21] M. Griswold, P. Jakob, R. Heidemann, M. Nittka, V. Jellus, J. Wang, B. Kiefer, and A. Haase, "Generalized Autocalibrating Partially Parallel Acquisitions (GRAPPA)," *Magnetic Resonance in Medicine*, vol. 47, pp. 1202–1210, 2002.

[22] M. Lustig, D. L. Donoho, J. M. Santos, and J. M. Pauly, "Compressed Sensing MRI," *IEEE Signal Processing Magazine*, vol. 25(2), pp. 72–82, 2008.

[23] Cishen Zhang and Ifat-Al-Baqee, "Parallel magnetic resonance imaging reconstruction by convex optimization", 2013 Third International Conference on Innovative Computing Technology (INTECH)in LONDON (IEEE Xplore), pp. 473-478, 2013.

[24] T. Goldstein and S. Osher, "The split Bregman method for l1 -regularized problems", *SIAM Journal of Imaging Science*, vol. 2, pp. 323–343, 2009.

[25]"Cartesian Dataset of Human Brain", http://maki.bme.ntu.edu.tw, 2005 (accessed in September 2019).

[26] "Precision Additive White Gaussian Noise Generator", http://dbmcorp.com/wp-content/uploads/2013/09/wgn.pdf, (accessed in June 2015).

[27] O. Dietrich, J. G. Raya, B. Reeder, F. M. Reiser, and S. O. Schoenberg, "Measurement of Signal-to-Noise Ratios in MR Images: Influence of Multichannel Coils, Parallel Imaging, and Reconstruction Filters", *Journal of Magnetic Resonance Imaging*, vol. 26, pp. 375–385, 2007.

Ifat A. Baqee was born in Dhaka, Bangladesh. Dr. Baqee completed his Bachelor of Science in Electrical, Electronic and Communication Engineering from Military Institute of Science and Technology (MIST), Mirpur, Dhaka under Bangladesh University of Professionals (BUP) in February 2009. After that, Dr. Baqee completed his Doctor of Philosophy (PhD) from the Swinburne University of Technology, Australia in 2016. The author's major field of study during the PhD tenure was computational image processing in the medical domain. After graduation, he first joined as a Lecturer at Stamford University Bangladesh in 2009. He served there up to 2012. After that, he moved to Australia to pursue his PhD degree. After completion of PhD, he came back to Bangladesh and joined as an Assistant Professor at the American International University Bangladesh (AIUB), Dhaka. He served up to 2019 in AIUB and then joined Southeast University, Dhaka, Bangladesh. He is currently serving there as an Assistant Professor in the EEE Department. His previous and current research interests include but are not limited to computational image processing, neural processing, medical instrumentation, power system automation, control system, etc. He has a good number of international journal and conference paper publications under his name.

Dr. Baqee is currently a member of the International Association of Computer Science and Information Technology (IACSIT) and also an active editorial member of the Australian Journal of Engineering and Innovative Technology (AJEIT).